Pergamon

Tetrahedron 58 (2002) 3647–3654

TETRAHEDRON

Synthesis and conformation of 3,10-di(*t*-butyl)- and 3,10-dichloro-4,9-methanothia[11]annulenes

Ryuta Miyatake, Shigeyasu Kuroda,* Takanori Kajioka,† Akihide Taketani and Mitsunori Oda*

Department of Applied Chemistry, Faculty of Engineering, Toyama University, Gofuku 3190, Toyama 930-8555, Japan

Received 6 March 2002; accepted 29 March 2002

Abstract—First two derivatives of 4,9-methanothia[11]annulene, 3,10-di(*t*-butyl)- and 3,10-dichloro-4,9-methanothia[11]annulenes (**4** and **5**), were synthesized from the diketosulfide **6**. Spectroscopic properties and X-ray crystallographic analyses revealed that **4** exists as an *anti*-conformer in respect of stereochemical relationship between the methano bridge and the sulfur atom both in solid state and in solution, while **5** exists as a *syn*-conformer in similarity to the parent of 4,9-methanothia[11]annulene (**3**).

Thiaannulenes having medium- to large-sized rings,[1,2] vinylogs of thiophene, enjoy flexibility with the various conformations and, thus, the non-planar structure of those molecules resulted in their atropic nature and labile chemical behavior.[1,2] For example, the thia[11]anulenes **1** and **2**, synthesized by Sondheimer and co-workers, did not show any ring current effect and the latter underwent facile electrocyclization of the triene part.[3] Introduction of a triple bond[4] or a bridge with either a methano group[5] or hetero-atom[6] into the annulene framework imposes less mobility upon the molecule. In 1972, Vogel and co-workers succeeded in the synthesis of the methano bridged annulene, 4,9-methanothia[11]annulene (**3**). Although **3** can adopt *syn* and *anti* conformations in respect of stereochemical relationship between the methano bridge and the sulfur atom based on inspection of Dreiding models, spectroscopic data of **3** document that it has the *syn* conformation and thereby shows atropic nature.[5] In this paper, we describe the synthesis, spectroscopic properties, and crystallographic analysis of first derivatives of **3**, 3,10-di(*t*-butyl)- and 3,10-dichloro-4,9-methanothia[11]annulenes (**4** and **5**), revealing their conformations both in solution and solid state (Chart 1, Fig. 1).

1. Results and discussion

1.1. Synthesis and spectroscopic properties of 3,10-di-(*t*-butyl)- and 3,10-dichloro-4,9-methanothia[11]-annulenes (4 and 5)

Synthesis of two 3,10-disubstituted derivatives was accomplished from the diketosuifide **6**[7] in a short step, which is different from the Vogel's method for the parent

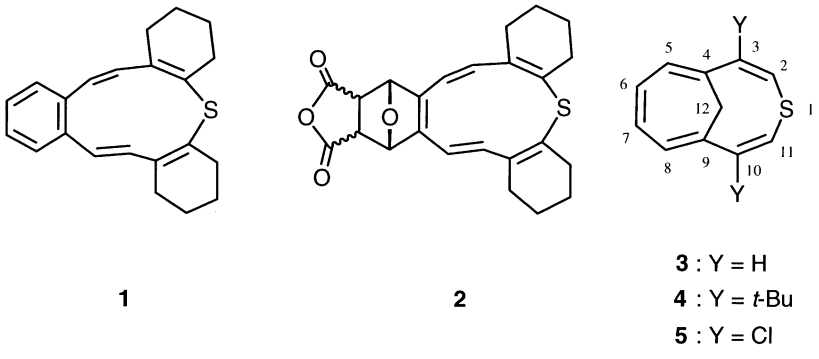

1 **2**

3 : Y = H
4 : Y = *t*-Bu
5 : Y = Cl

Chart 1.

Keywords: annulenes; heterocycles; conformation; X-ray crystal structures; density functional calculation.

* Corresponding authors. Address: Department of Materials Chemistry, Faculty of Engineering, Toyama University, Gofuku 3190, Toyama 930-8555, Japan. Tel.: +81-76-445-6820; fax: +81-76-445-6819; e-mail: kuro@eng.toyama-u.ac.jp; oda@eng.toyama.u.ac.jp

† Present address: Toyota Central R&D Labs, Nagakute, Aichi 480-1192, Japan.

0040–4020/02/$ - see front matter
PII: S0040-4020(02)00353-8

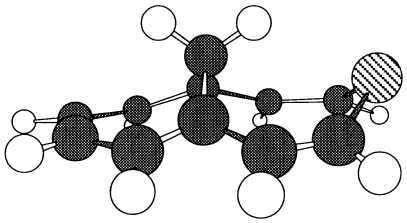

3

Figure 1. The optimized structure (Chem3D output) of **3** at the BLYP/6-31G* level of theory.

1 (Scheme 1). Compound **6** was reacted with an excess of *t*-BuMgCl in THF to give the unstable diol. Dehydration of this diol was examined under various reaction conditions, as shown in Table 1. Although the reactions with phosphorus oxychloride in pyridine and the Burgess reagent[8] as a dehydration reagent gave **4** in poor yields based on **3**, **4** was obtained in a slightly better yield (10%) under the conditions with thionyl chloride in pyridine. Acidic dehydration with *p*-toluenesulfonic acid in benzene gave none of **4**. Compound **5** was synthesized directly from **6** with phosphorous pentachloride. The best yield (12% yield) of **5** was observed under the conditions with an excess

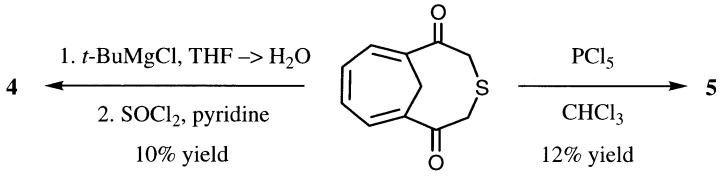

Scheme 1.

Table 1. Results of dehydration of the diol, prepared from **6** and *t*-butylmagnesium chloride, under various reaction conditions

Entry	Reagent/solvent	Reaction conditions	Yield (%) of **4**[a]
1	$POCl_3$/pyridine	60°C/1 h	4
2	$SOCl_2$/pyridine	60°C/0.5 h	10
3	*p*-TsOH/PhH	50°C/3 h	0
4	Burgess/THF	50°C/3 h	3
5	Burgess/PhH	70°C/2 h	7

[a] The isolated yield based on **6**.

of phosphorous pentachloride under reflux in chloroform for 2 h. The reaction conditions for longer reaction period of the reaction resulted in desulfurization of **5** (vida infra).

Selected spectrosopic data of **3**–**5** are shown in Fig. 2. The critical differences between them were shown in the chemical shift value of one of the methylene hydrogens and absorption wavelength in the UV absorption spectrum. The H_α of **4** in the ^1H NMR spectrum appears at normal aliphatic region (δ=2.54 ppm), while the H_a and H_A of **3**

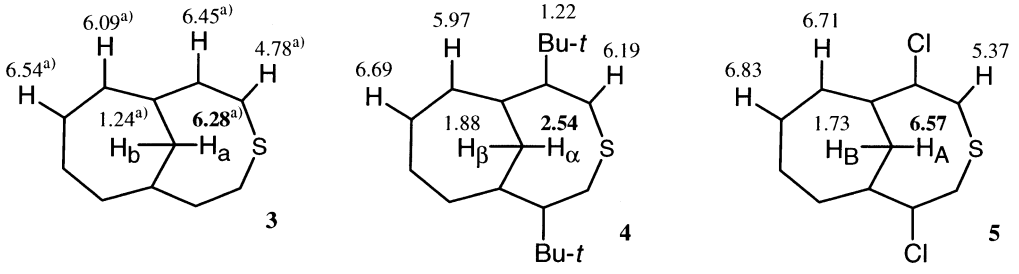

Figure 2. ^1H NMR chemical shifts (δ (ppm) in chloroform-*d*) and UV absorption maxima (log ε in parentheses) of **3**–**5**. (a) Taken from Ref. 5.

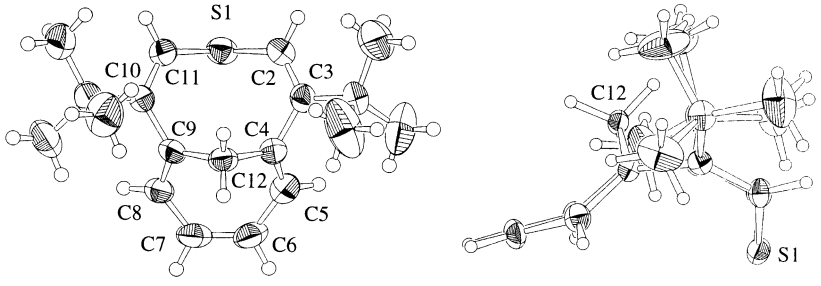

Figure 3. The ORTEP drawings of one of two independent structures in the crystal of the methanothia[11]annulene **4**.

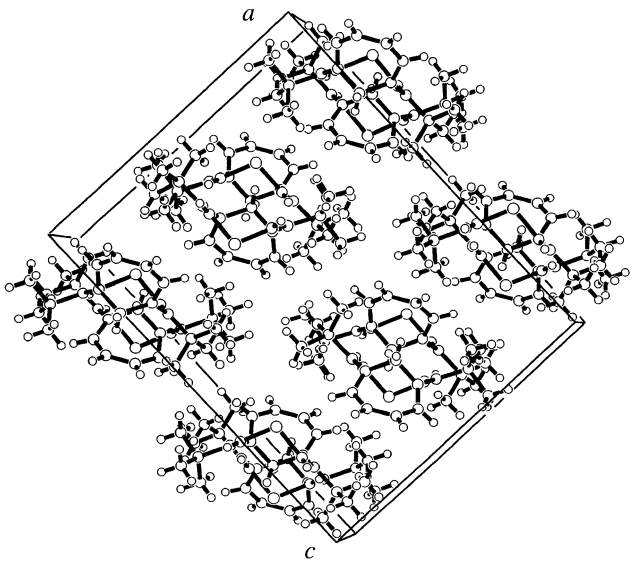

Figure 4. The crystal packing of the methanothia[11]annulene **4**. A view from *b* axis.

and **5** resonate at abnormally low field (δ=6.28 and 6.57 ppm, respectively). The latter phenomenon was reasonably explained by combined effects of the diamagnetic anisotropy of the sulfur–carbon bonds and the field effect and a steric compression of the sulfur atom, as reported by Vogel.[5] Thus, the chemical shift value of H_α indicates that this hydrogen atom is distant from the sulfur atom in the molecular structure of **4**, presenting that **4** has a conformation different from **3** and **5**. Although ^{1}H NMR spectra of **4** and **5** were recorded at a range of temperatures between −100 and +100°C with either a mixture of dichloromethane-d_2 and carbondisulfide, chloroform-*d*, or dimethylsulfoxide-d_6 as solvent, any dynamic behavior, such as ring flipping and cycloheptatriene–norcaradiene equilibrium, was not observed. The UV spectrum of **4** with only shoulder absorptions at 248 and 279 nm differs from those of **3**, **5**, and the corresponding hydrocarbon, bicyclo[5.4.1]dodeca-2,5,7,9,11-pentaene (λ_{max}=248 and 327 nm), and its long wavelength maximum is rather close to that (λ_{max}=245 nm) of 1,6-bis(hydroxymethy)-1,3,5-cycloheptatriene.[9] Thus, the triene part of the seven-

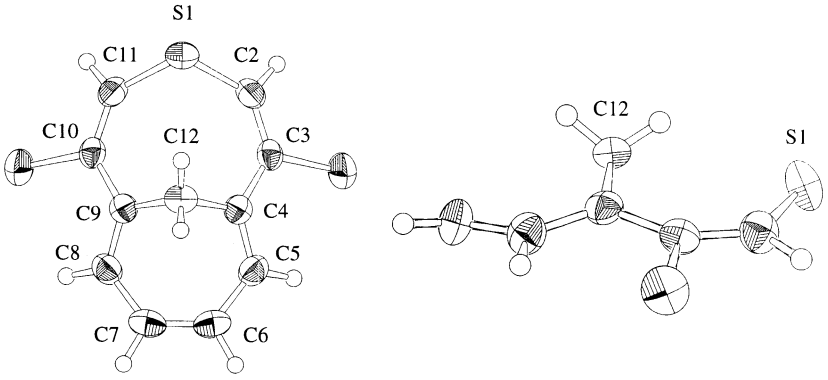

Figure 5. The ORTEP drawings in the crystal of the methanothia[11]annulene **5**.

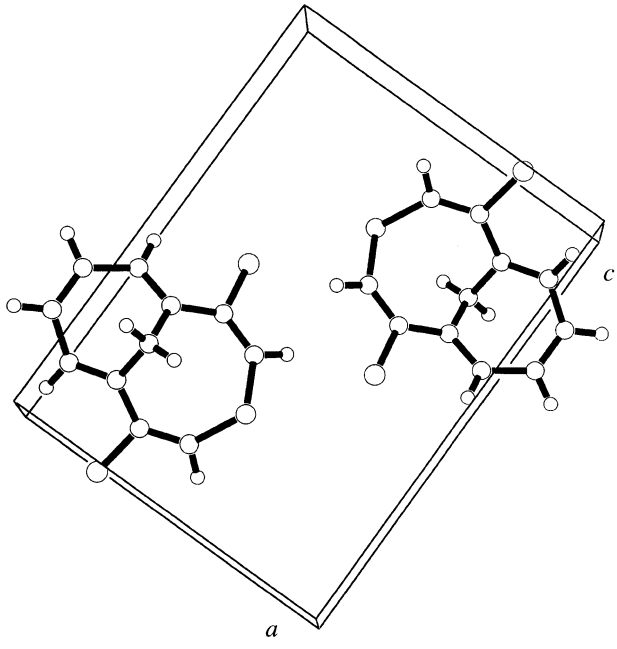

Figure 6. The crystal packing of the methanothia[11]annulene **5**. A view from *b* axis.

membered ring is indicated to be disconnected from the divinyl sulfide part and the former moiety mainly contributes the long wavelength absorption. From these spectroscopic data, it is concluded that in solution **4** exists entirely as an *anti*-conformer in which a large torsion angle through the C2–C3–C4–C5 (or C8–C9–C10–C11) carbons is expected, while **5** as a *syn*-conformer with its effective π-conjugation through the pentaene part.

1.2. X-Ray crystal structures of 4 and 5

The molecular structures of **4** and **5** were further elucidated by X-ray crystallographic analysis. ORTEP drawings and the crystal packing are shown in Figs. 3–6, respectively. There are two independent molecules with C_1 symmetry in the crystal of **4** with very little differences in the bond lengths.[10] As clearly shown in Fig. 3, **4** has the *anti*-conformation with the average non-bonded atomic distance of 3.51 Å between the sulfur and the C12 carbon atoms. Their thiaanulene rings of these two molecules are facing each other in the opposite direction with the sulfur atoms inside and the methano bridges outside in the crystal (Fig. 4). As expected above, average torsion angles for the C2–C3–C4–C5 and C7–C8–C9–C10 carbons of the two molecules

Table 2. Selected bond lengths of the crystal structures of **4** and **5** and differences thereof

Bond	Length (Å) in **4**[a]	Length (Å) in **5**	Δ (**5**–**4**)
S1–C2	1.793	1.773(2)	−0.020
S1–C11	1.780	1.773(2)	−0.007
C2–C3	1.327	1.337(3)	0.010
C3–C4	1.480	1.459(3)	−0.021
C4–C5	1.348	1.359(3)	0.011
C5–C6	1.436	1.442(4)	0.006
C6–C7	1.354	1.342(6)	–0.012
C7–C8	1.445	1.442(4)	−0.003
C8–C9	1.344	1.359(3)	0.015
C9–C10	1.487	1.459(3)	−0.028
C10–C11	1.335	1.337(3)	0.002
C4–C12	1.502	1.497(3)	−0.005
C9–C12	1.506	1.497(3)	−0.009

[a] Average values of two independent molecules in the crystal.

are 79.4 and 77.1°, respectively, which are large enough to disconnect the π-conjugation between the cycloheptatriene and the divinyl sulfide parts.

The X-ray structure of **5** shows C_s symmetry and has the *syn* conformation with the non-bonded atomic distance of 3.12 Å between the sulfur and the C12 carbon atoms (Fig. 5). The torsion angle for the C2–C3–C4–C5 carbons of **5** is 17.9° in contrast to the case of **4**. Table 2 shows bond lengths in the thiaannulene rings of **4** and **5** and differences in them. The C3–C4 and C9–C10 bonds of **4** are longer than those of **5**, also indicating dissimilarity of p-orbital overlap at there. From these structural data, it is clearly revealed that the di(*t*-butyl) derivative **4** exists as an *anti*-conformer and the dichloro derivative **5** exists as a *syn*-conformer both in solution and in solid state.

It should also be noted that non-bonded carbon–carbon distances at the methano-bridges in their crystal structures of **4** and **5** are 2.84 and 2.85 Å long, respectively. Thus, the C4–C9 interaction is negligible.[11]

1.3. Density functional calculations of 4 and 5

The density functional calculations at BLYP/6-31G* level of theory on **4** and **5** support these spectroscopic and X-ray crystallographic findings. Although a optimized structure of a *syn*-conformer and none of an *anti*-conformer for **3** was obtained, those of *syn*- and *anti*-conformers for **4** and **5** were obtained (Fig. 7).[12] Thus, **3** is suggested to have a single-well potential in contrast to the inspection by Drieding models, while **4** and **5** have has a double-well potential.

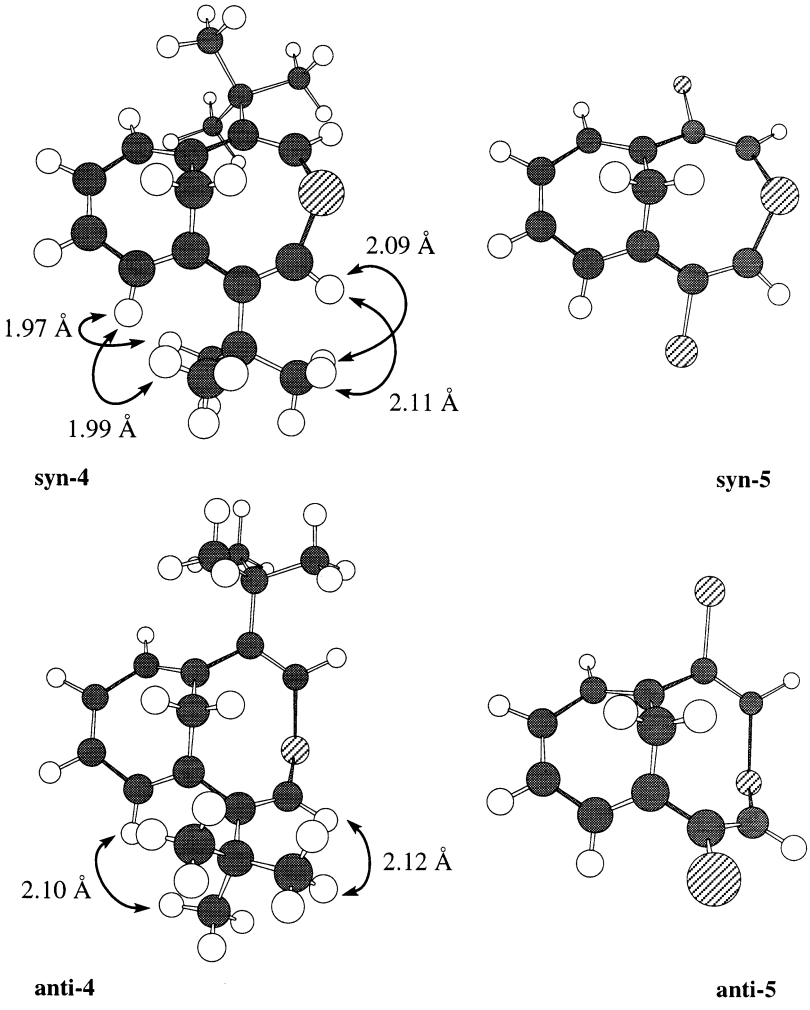

Figure 7. Optimized structures (Chem3D output) of *syn*- and *anti*-conformers for **4** and **5** at the BLYP/6-31G* level of theory and selected short non-bonded atomic distances.

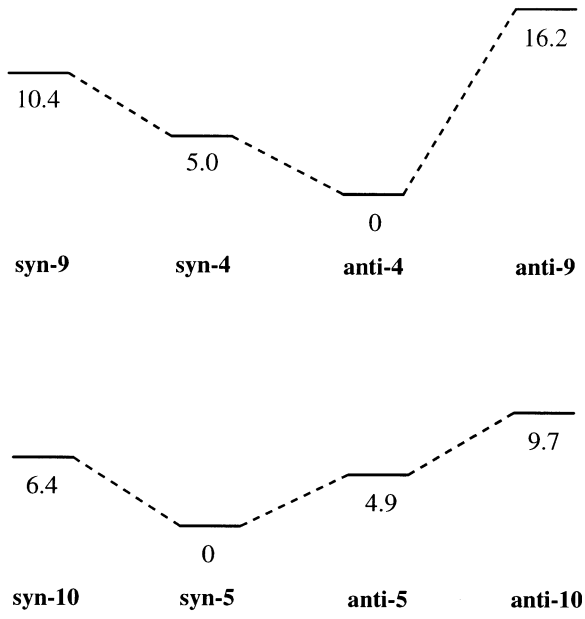

Figure 8. Relative total energies (in kcal mol^{-1}) of optimized *syn*- and *anti*-structures for **4**, **5**, **9**, and **10** at the BLYP/6-31G* level of theory.

The *anti*-conformer of **4** is predicted to be more stable than the *syn*-conformer by 5.0 kcal mol^{-1}, and the *anti*-conformer of **5** less stable than the *syn*-conformer by 4.9 kcal mol^{-1}, supporting experimental facts. Steric repulsion between the hydrogen atoms at the 5 and 8 positions in the *syn*-conformer and the *t*-butyl groups accounts for its instability; the non-bonded atomic distances between the hydrogens at the 5 and 8 positions and the closest ones of the *t*-butyl groups are 1.97 and 1.99 Å in the optimized structure of the *syn*-conformer. No such short non-bonded atomic distance less than 2.0 Å is observed in the *anti*-conformer.

1.4. Desulfurization of 4 and 5

The conformational difference between **4** and **5** is reflected in their chemical behavior. Although the parent **1** was reported to undergo desulfurization at 50°C, **4** and **5** were reluctant to that at the same temperature. Compound **5** gradually undergoes desulfurization above 80°C and **4** above 120°C to give the corresponding 2,5-disubstituted 1,6-methano[10]annulenes, **7** and **8**, quantitatively. At 120°C in dimethylsulfoxide-d_6, half life times of **4** and **5** were measured by NMR analysis to be 3.75 h and 9.2 min, respectively. As speculated in cases of **3** and thiepins, their episulfide isomers **9** and **10** are a most probable intermediate in these sulfur extrusion reactions. In a process of electrocyclization forming episufides, distance of the bond-forming carbon atoms is an important factor to evaluate prospects of the reaction. However, non-bonded distance between the C2 and C11 carbon atoms in crystal structures of **4** (2.84 Å) is similar to that (2.85 Å) of **5**, as unaware of difference of the reactivity between them. The reluctance of **4** in desulfurization can be attributed to relative instability of the episulfides, *syn*-**9** and *anti*-**9**, to **4**, compared with the case between **5** and **10**, based on density functional calculations at the BLYP/6-31G* level of theory (Fig. 8),[13] though calculations of transition states for these possible processes have not been achieved yet (Scheme 2).

It is worthy to note that this synthetic sequence from these methanothia[11]annulenes to **7** and **8** provides another route to 2,5-disubstituted 1,6-methano[10]annulene in addition to our previous method.[9]

2. Summary

In conclusion, we have synthesized two derivatives of **3**, 3,10-di(*t*-butyl)- and 3,10-dichloro-4,9-methanothia[11]-annulene (**4** and **5**) by a route in a short step from diketosulfide **6**. Spectroscopic data and X-ray crystallographic analysis evidence that the former derivative exists as an *anti*-conformer both in solid state and in solution in contrast to the case of the parent **1** and the latter derivative which exist as the *syn*-conformer. The conformational difference between **4** and **5** is reflected in their desulfurization. The density functional calculations for both conformers for **4** suggest that the *syn*-conformer is disfavored because of the steric repulsion between the hydrogens at the 5 and 8 positions and the *t*-butyl groups.

3. Experimental

3.1. General

Melting points were measured on a Yanaco MP-3 and are uncorrected. IR spectra were recorded on a JASCO IR-810 and Perkin–Elmer Spectrum RX I spectrometers. UV spectra were measured on a Shimadzu UV-1600 spectrometer. ^{1}H NMR (400 MHz) and ^{13}C NMR (100 Hz) were recorded with tetramethylsilane as an internal standard on a JEOL α400. Mass spectra were measured on JEOL JMS-D-300 and JEOL GC-Mate mass spectrometers. Column

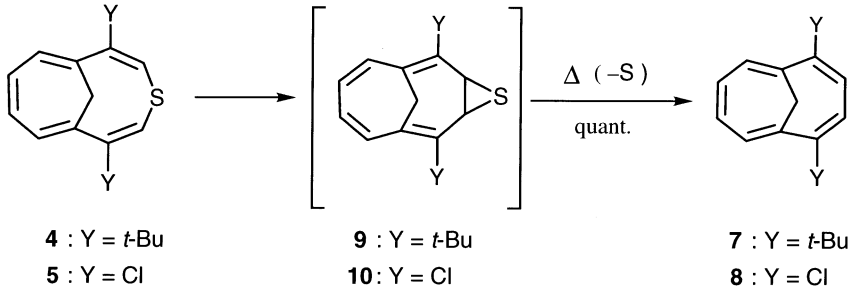

4 : Y = *t*-Bu
5 : Y = Cl

9 : Y = *t*-Bu
10: Y = Cl

7 : Y = *t*-Bu
8 : Y = Cl

Scheme 2.

chromatography was done with Merck Kieselgel 60 Art 7734. Ethyl ether and THF were purified just before use by distillation from sodium diphenylketyl under a nitrogen atmosphere. A solution of *t*-butylmagnesium chloride in ether was purchased from Tokyo Kasei Inc. and was titrated before use. The density functional calculations were done by using the MULLIKEN (ver. 2.0.0, 1995, IBM Co.) on an IBM RS/6000-397 computer.

3.1.1. Synthesis of 3,10-di(*t*-butyl)-4,9-methanothia[11]-annulene (4). A solution of **6** (1.00 g, 4.85 mmol) in 30 ml of THF was added dropwise to a 1.25 M solution of *t*-butylmagnesium chloride in ether (15.5 ml, 19.4 mmol) at room temperature. After being stirred for 3 h, the reaction mixture was carefully poured into a saturated ammonium chloride solution (100 ml) and extracted with ether (50 ml×3). The combined organic layer was washed with brine, and dried with anhydrous $MgSO_4$. After evaporation of the solvent, the residual oil was dissolved in 20 ml of pyridine. To this solution was added dropwise 1.40 ml of thionyl chloride. This mixture was heated at 60°C for 0.5 h, and was then poured into ice-water and extracted with ether (40 ml×3). The combined organic layer was washed with water and brine and dried with anhydrous $MgSO_4$. After evaporation of the solvent, the residue was purified by silica gel chromatography to give 160 mg (10% yield) of **4** as faint yellow needles. Mp=73–75°C. ^{1}H NMR ($CDCl_3$) δ=1.22 (s, 18H), 1.88 (d, J=11.2 Hz, 1H), 2.54 (d, J=11.2 Hz, 1H), 5.97 (m, 2H), 6.19 (s, 2H), 6.69 (m, 2H); ^{13}C NMR ($CDCl_3$) δ=29.0 ($C(CH_3)_3$), 38.1 (CH_2), 43.8 ($C(CH_3)_3$), 115.4 (C-2,11), 121.5 (C-6,7), 128.7 (C-5,8), 129.7 (C-4,9), 167.5 (C-3,10). IR (KBr) ν (cm^{-1}) 3037w, 3006s, 2965s, 2954s, 2903m, 2865m, 1571w, 1520w, 1478m, 1459m, 1425m, 1360m, 1313w, 1236w, 1198w, 1068w, 989w, 857w, 841w, 828m, 741s, 703m; MS (70 eV) *m/z* (rel. intensity) 286 (M^+, 27), 271 (3), 229 (6), 215 (16), 197 (5), 173 (24), 115 (7), 91 (4), 77 (4), 54 (100); UV λ_{max} (hexane, nm) 248sh (log ε=3.79), 279sh (3.50). Found: C, 79.35; H, 9.16%. Calcd for $C_{19}H_{26}S$: C, 79.66; H, 9.15%.

3.1.2. Synthesis of 3,10-dichloro-4,9-methanothia[11]-annulene (5). To a solution of **6** (0.500 g, 2.43 mmol) in 30 ml of chloroform was added 1.77 g (8.51 mmol) of phosphorous chloride. After being refluxed for 2 h, the reaction mixture was carefully poured into ice-water (80 ml) and extracted with dichloromethane (30 ml×3). The combined organic layer was washed with a saturated sodium bicarbonate solution and brine, and dried with anhydrous $MgSO_4$. After evaporation of the solvent, the residual oil was purified by silica gel chromatography to give 74 mg (12% yield) of **5** as orange needles. Mp=124–126°C. ^{1}H NMR ($CDCl_3$) δ=1.73 (d, J=13.2 Hz, 1H), 5.37 (s, 2H), 6.57 (d, J=13.2 Hz, 1H), 6.73 (m, 2H), 6.83 (m, 2H); ^{13}C NMR ($CDCl_3$) δ=27.6 (CH_2), 106.8 (C-2,11), 120.7 (C-4,9), 127.9 (C-5,8), 131.8 (C-6,7), 137.9 (C-3,10). IR (KBr) ν (cm^{-1}) 3040m, 3015m, 1528m, 1445s, 1120s, 1063s, 968s, 885s, 800s, 719s; MS (70 eV) *m/z* (rel. intensity) 246 (M^+, 9), 244 (M^+, 29), 242 (M^+, 39), 209 (59), 207 (47), 209 (29), 198 (22), 196 (39), 175 (78), 173 (26), 172 (74), 171 (100), 162 (29), 139 (47), 128 (20), 127 (29), 85 (20), 63 (27); UV–Vis λ_{max} (hexane) 242 nm (log ε=4.40), 287 (4.34), 397 (2.52). Found: C, 54.33; H, 3.42%. Calcd for $C_{11}H_8Cl_2S$: C, 54.34; H, 3.32%.

3.1.3. Synthesis of 2,5-di(*t*-butyl)-1,6-methano[10]annulene (7). A solution of **4** (40.0 mg, 0.14 mmol) in 10 ml of DMSO was heated at 120°C for 12 h. The reaction mixture was poured into water (30 ml) and extracted with hexane (10 ml×3). The combined organic layer was washed with brine, and dried with anhydrous $MgSO_4$. After evaporation of the solvent, the residual oil was purified by silica gel chromatography to give 35 mg (99% yield) of **7** as a pale yellow oil. ^{1}H NMR ($CDCl_3$) δ=−1.00 (d, J=9.6 Hz, 1H), −0.26 (d, J=9.6 Hz, 1H), 1.54 (s, 18H), 6.96 (s, 2H), 7.24 (m, 2H), 7.64 (m, 2H); ^{13}C NMR ($CDCl_3$) δ=32.9 ($C(CH_3)_3$), 37.2 ($C(CH_3)_3$), 37.9 (CH_2), 117.0 (C-1,6), 123.5 (C-3,4), 126.2 (C-8,9), 126.5 (C-7,10), 150.6 (C-2,5). IR (liq. film) ν (cm^{-1}) 3030w, 2950s, 2895s, 2865s, 1480m, 1460m, 1395w, 1383w, 1365s, 1300w, 1265w, 1230m, 1200m, 1178w, 1155w, 1115w, 1025w, 933w, 905w, 835m, 818w, 758s, 718s, 665m; MS (70 eV) *m/z* (rel. intensity) 254 (M^+, 27), 239 (19), 198 (22), 197 (84), 183 (48), 169 (38), 167 (18), 165 (189, 155 (28), 141 (38), 129 (10), 128 (11), 115 (10), 69 (14), 57 (100); UV λ_{max} (methanol) 260 nm (log ε=4.11), 312 (3.30). Found: *m/z* 254.2019. Calcd for $C_{19}H_{26}$: M, 254.2032.

3.1.4. Synthesis of 2,5-dichloro-1,6-methano[10]annulene (8). A solution of **5** (30.0 mg, 0.123 mmol) in 10 ml of toluene was heated at 100°C for 1 h. After evaporation of the solvent, the residual oil was purified by silica gel chromatography to give 25 mg (98% yield) of **8** as a pale yellow oil. ^{1}H NMR ($CDCl_3$) δ=−0.52 (d, J=10.5 Hz, 1H), −0.12 (d, J=10.5 Hz, 1H), 7.09 (s, 2H), 7.35 (m, 2H), 7.75 (m, 2H); ^{13}C NMR ($CDCl_3$) δ=33.1 (CH_2), 113.2 (C-1,6), 127.1 (C-3,4), 127.9 (C-2,5), 129.0 (C-7,10), 129.3 (C-8,9). IR (liq. film) ν (cm^{-1}) 3010w, 2920s, 1443m, 1380m, 1110s, 980m, 892m, 798w, 752m, 708s; MS (70 eV) *m/z* (rel. intensity) 214 (M^+, 6), 212 (M^+, 14), 210 (M^+, 21), 177 (100), 176 (14), 175 (32), 149 (16), 148 (16), 139 (51), 87 (12), 70 (11), 63 (14); UV λ_{max} (methanol) 263 nm (log ε=4.31), 324 (3.50). Found: *m/z* 210.0005. Calcd for $C_{11}H_8{}^{35}Cl_2$: M, 210.0002.

3.2. Measurements of a half life time in desulfurization of 4 and 5 by NMR spectroscopy

A solution of the methanothia[11]annulene (ca. 0.1 mmol) and dichloromethane (ca. 0.05 mmol) as an internal standard in DMSO-d_6 was charged in an NMR tube, which then was sealed. At a probe temperature of 120°C, the molecular decay was measured with signals of the *t*-butyl group for **4** and one, at δ 1.73 ppm, of the bridging methylene protons for **5**.

3.3. X-Ray structure analysis of the thia[11]annulene 4

Faint yellow prismatic crystals of **4** were obtained by recrystallization from a mixture of water and methanol. One of them having approximate dimensions of 0.50×0.50×0.50 mm^3 was mounted on a glass fiber. All measurements were made on a Rigaku AFC7R diffractometer with graphite monochromated Mo Kα radiation and a rotating anode generator. Cell constants and an orientation matrix for data collection, obtained from a least-squares refinement using the setting angles of 25 carefully centered reflections in the range $22.26<2\theta<28.68°$,

corresponded to a primitive monoclinic cell with dimensions: a=14.448 (3) Å, b=12.927 (4) Å, c=18.743 (3) Å, β=89.83 (2)°, V=3500 (1) Å^3. For Z=8 and formula weight=286.47, the calculated density is 1.09 g cm^{-3}. Based on the systematic absences of $h01$: $l\neq 2n$, $0k0$: $k\neq 2n$, the space group was uniquely determined to be $P2_1/c$ (# 14). The data were collected at a temperature of 23°C using the $\omega-2\theta$ scan technique to a maximum 2θ value of 60.0°. Omega scans of several intense reflections, made prior to data collection, had an average width at half-height of 0.26° with a take-off angle of 6.0°. Scans of $(1.52+0.30\tan\theta)$° were made at speed of 32.0° min^{-1} (in omega). The weak reflections ($I<10.0\sigma(I)$) were rescanned (maximum of 5 scans) and the counts were accumulated to ensure good counting statistics. Stationary background counts were recorded on each side of the reflection. The ratio of peak counting time to background counting time was 2:1. The diameter of the incident beam collimator was 0.5 mm and the crystal to detector distance was 235 mm. The computer-controlled slits were set to 3.0 mm (horizontal) and 3.0 mm (vertical). Of the 11,009 reflections which were collected, 10,204 were unique (R_{int}=0.027). The intensities of three representative reflections were measured after every 150 reflections. No decay correction was applied. The structure was solved by direct methods and expanded using Fourier techniques. The non-hydrogen atoms were refined anisotropically. Hydrogen atoms were included but not refined. The final cycle of full-matrix least-squares refinement was based on 2502 observed reflections ($I>3.00\sigma(I)$) and 361 variable parameters and converged (largest parameter shift was 0.00 times its esd) with unweighted and weighted agreement factors of: R=0.054, Rw=0.062, and $R1$=0.054 for $I>3.0\sigma(I)$ data. The standard deviation of an observation of unit weight was 1.65. The weighting scheme was based on counting statistics and included a factor (p=0.031) to downweight the intense reflections. Plots of $\sum w(|F_0|-|F_c|)^2$ versus $|F_0|$, reflection order in data collection, $\sin\theta/\lambda$ and various classes of indices showed no unusual trends. The maximum and minimum peaks on the final difference Fourier map corresponded to 0.18 and -0.21 e$^-$ Å^{-3}, respectively. Tables of fractional atomic coordinates, thermal parameters, bond lengths and angles have been deposited at the Cambridge Crystallographic Data Center, 12 Union Road, Cambridge CB2 1EZ, UK (CCDC 166383).

3.4. X-Ray structure analysis of the thia[11]annulene 5

An orange prismatic crystals of **5** with dichloromethane were obtained by recrystallization from a mixture of hexane and dichloromethane. One of them having approximate dimensions of 0.30×0.30×0.50 mm^3 was mounted on a glass fiber. All measurements were made on a Rigaku AFC7R diffractometer with graphite monochromated Mo Kα radiation and a rotating anode generator. Cell constants and an orientation matrix for data collection, obtained from a least-squares refinement using the setting angles of 25 carefully centered reflections in the range $27.23<2\theta<29.83$°, corresponded to a primitive monoclinic cell with dimensions: a=4.332(2) Å, b=12.714(1) Å, c=9.518(1) Å, β=95.87(2)°, V=521.4(2) Å^3. For Z=2 and formula weight=243.15, the calculated density is 1.55 g cm^{-3}. Based on the systematic absences of $0k0$: $k\neq 2n$, packing considerations, a statistical analysis of intensity distribution, and the successful solution and refinement of the structure, the space group was determined to be $P2_1/m$ (#11). The data were collected at a temperature of 23°C using the $\omega-2\theta$ scan technique to a maximum 2θ value of 60.0°. Omega scans of several intense reflections, made prior to data collection, had an average width at half-height of 0.26° with a take-off angle of 6.0°. Scans of $(1.78+0.30\tan\theta)$° were made at speeds of 32.0° min^{-1} (in omega). The weak reflections ($I<10.0\sigma(I)$) were rescanned (maximum of 5 scans) and the counts were accumulated to ensure good counting statistics. Stationary background counts were recorded on each side of the reflection. The ratio of peak counting time to background counting time was 2:1. The diameter of the incident beam collimator was 0.5 mm and the crystal to detector distance was 235 mm. The computer-controlled slits were set to 3.0 mm (horizontal) and 4.0 mm (vertical). Of the 1771 reflections which were collected, 1579 were unique (R_{int}=0.013). The intensities of three representative reflections were measured after every 150 reflections. No decay correction was applied. The structure was solved by direct methods and expanded using Fourier techniques. The non-hydrogen atoms were refined anisotropically. Hydrogen atoms were included but not refined. The final cycle of full-matrix least-squares refinement was based on 2502 observed reflections ($I>3.00\sigma(I)$) and 361 variable parameters and converged (largest parameter shift was 0.00 times its esd) with unweighted and weighted agreement factors of: R=0.035, Rw=0.042, and $R1$=0.035 for $I>3.0\sigma(I)$ data. The standard deviation of an observation of unit weight was 1.34. The weighting scheme was based on counting statistics and included a factor (p=0.030) to downweight the intense reflections. Plots of $\sum w(|F_0|-|F_c|)^2$ versus $|F_0|$, reflection order in data collection, $\sin\theta/\lambda$ and various classes of indices showed no unusual trends. The maximum and minimum peaks on the final difference Fourier map corresponded to 0.24 and -0.30 e$^-$ Å^{-3}, respectively. Tables of fractional atomic coordinates, thermal parameters, bond lengths and angles have been deposited at the Cambridge Crystallographic Data Center, 12 Union Road, Cambridge CB2 1EZ, United Kingdom (CCDC 175924).

Acknowledgements

This work was supported financially by a Grant-in-Aid Scientific Research (No. 10640513 to S. K. and No. 13640528 to M. O.) from the Ministry of Education, Science, Culture and Sports, Japan. We thank Dr Shengli Zuo and Mr Shinji Furuta at Toyama University for their technical assistance for the preparation of compounds **4**–**6**.

References

1. Nakagawa, M. *The Chemistry of Annulene*, Vol. 4; Osaka University: Osaka, 1996; Chapter 4, pp 189–238 and Chapter 7, pp 371–412.
2. Balaban, A. T.; Banciu, M.; Ciorba, V. *Annulenes. Benzo-, Hetero-, Homo-Derivatives and Their Valence Isomers*, Vol. III; CRC: Boca Raton, FL, 1987; pp 1–80.

3. Holmes, A. B.; Sondheimer, F. *J. Am. Chem. Soc.* **1970**, *92*, 5284–5285. Holmes, A. B. Sondheimer. *Chem. Commun.* **1971**, 1434–1436.
4. Wife, R. L.; Sondheimer, F. *J. Am. Chem. Soc.* **1975**, *97*, 640–641. Ojima, J.; Nagaya, M.; Katsuyama, G.; Yamamoto, G. *J. Chem. Soc., Perkin Trans. 1* **1990**, 869–879.
5. Vogel, E.; Feldmann, R.; Duwel, H.; Cremer, H.-D.; Guther, H. *Angew. Chem.* **1972**, *84*, 207–208 *Angew. Chem. Int. Ed. Engl.*, **1972**, *11*, 217–218.
6. Ogawa, H.; Shimojo, N. *Tetrahedron Lett.* **1972**, 4129–4132.
7. Kuroda, S.; Oda, M.; Kuramoto, S.; Mizukami, Y.; Shimao, I. *Tetrahedron Lett.* **1994**, *35*, 7405–7408. Kuroda, S.; Oda, M.; Kuramoto, S.; Fukuta, A.; Mizukami, Y.; Miyatake, R.; Izawa, M.; Shimao, I. *Tetrahedron Lett.* **1997**, *38*, 8291–8294. Zuo, S.; Kuroda, S.; Oda, M.; Kuramoto, S.; Mizukami, Y.; Fukuta, A.; Miyatake, R.; Shaheen, S. I.; Kajioka, T.; Kyogoku, M. *Heterocycles* **2001**, *54*, 159–170.
8. Burgess, E. D.; Penton, Jr., R. H.; Taylor, E. A. *J. Org. Chem.* **1973**, *38*, 26–31.
9. Kuroda, S.; Zuo, S.; Oda, M.; Fukuta, A.; Kajioka, T.; Saito, T.; Furuta, S.; Tsukumo, H.; Sano, K.; Miyatake, R.; Tomoda, S.; Hayakawa, C.; Nozawa, H. *Bull. Chem. Soc. Jpn.* **2000**, *73*, 1659–1671.
10. Differences in the C–C and C–S bond lengths between the two molecules are less than 0.013 Å for the bonds in the rings and 0.027 Å for the others.
11. Simonetta, M. *Pure Appl. Chem.* **1980**, *52*, 1597–1610.
12. Total energies were calculated as follows: −1137.397544 a.u. for the *anti*-conformer of **4**, −1137.389505 a.u. for the *syn*-conformer of **4**, −1742.261706 a.u. for the *anti*-conformer of **5**, and −1742.269578 a.u. for the *syn*-conformer of **5**.
13. Total energies were calculated as follows: −1137.371725 a.u. for the *anti* episulfide **9**, −1137.380971 a.u. for the *syn* episufide **9**, −1142.254106 a.u. for the *anti* episulfide **10**, and −11.42.259251 a.u. for the *syn* episulfide **10**.